

Limit State Analysis: upper/lower bounds approach to the computation of the limit load of a Von Mises rigid-plastic material body in plane stress.

Raymundo Cordero & Javier Bonet

*Civil & Computational Engineering Centre
School of Engineering
University of Wales Swansea
SA2 8PP*

cgorder@swansea.ac.uk; J.Bonet@swansea.ac.uk

Key words: limit analysis, upper/lower bounds, rigid-plastic, flux equilibration, adaptive

1. INTRODUCTION

This research work has its foundation on the classical theorems of Limit Analysis for the upper and lower bound approximation to the limit load of a Von Mises rigid-plastic incompressible material body in plane stress. The approach uses a Finite Element solution with a Newton-Raphson optimisation technique for the computation of an upper bound to the limit load. Then a flux equilibration technique based on Ladeveze constant flux is used to obtain equilibrated interelement tractions with which to compute a lower bound estimate to the collapse load from the localised problem, on an element-by-element basis. Both estimates are used in an adaptive scheme to produce a decreasing interval on which the true limit load lies.

2. GOVERNING EQUATIONS

Statically and kinematically admissible states are the core of the classic limit analysis bound theorems. These, as stated in [1] are as follows: a *statically admissible state* is described by a stress field σ_s and a load multiplier γ^s such that

$$-\text{div } \sigma_s = \gamma^s \mathbf{b} \text{ in } \Omega; \quad \sigma_s \mathbf{n} = \gamma^s \mathbf{t} \text{ on } \partial\Omega_t; \quad f(\sigma_s) \leq 0 \text{ in } \Omega$$

for body forces, \mathbf{b} , and given surface tractions, \mathbf{t} . Similarly, a *kinematically admissible state* is described by a displacement rate field $\dot{\mathbf{u}}_k$ and a plastic strain rate field $\dot{\boldsymbol{\epsilon}}$ such that

$$\dot{\boldsymbol{\epsilon}} = (\nabla \dot{\mathbf{u}}_k)_{\text{sym}} \text{ in } \Omega; \quad \dot{\mathbf{u}}_k = 0 \text{ in } \partial\Omega_u; \quad \int_{\Omega} \mathbf{b} \cdot \dot{\mathbf{u}}_k d\Omega + \int_{\partial\Omega_t} \mathbf{t} \cdot \dot{\mathbf{u}}_k ds > 0$$

From the power equality we can write the kinematically admissible multiplier as

$$\gamma^k = \int_{\Omega} D_p(\dot{\boldsymbol{\epsilon}}) d\Omega / \left(\int_{\Omega} \mathbf{b} \cdot \dot{\mathbf{u}}_k d\Omega + \int_{\partial\Omega_t} \mathbf{t} \cdot \dot{\mathbf{u}}_k ds \right)$$

Where $D_p(\dot{\boldsymbol{\epsilon}})$ is the plastic dissipation rate per unit volume. It can be shown that from the *Postulate of Maximum Plastic Dissipation* we can write the relation

$$\gamma^s \leq \gamma^k$$

This relation corresponds particularly to *rigid-plastic* materials as described in [2], in which $\dot{\boldsymbol{\epsilon}}$ is equal to $\dot{\boldsymbol{\epsilon}}^p$, neglecting the *elastic strain rate*, which is valid for this type of material. In order to build the constitutive relations consider a simple Von-Mises material. The rate of plastic dissipation for a given rate of the deformation tensor \mathbf{d} is given as:

$$D_p(\mathbf{d}) = \sigma_y \dot{\bar{\boldsymbol{\epsilon}}}(\mathbf{d}) \quad \text{with} \quad \mathbf{d} = \frac{1}{2}(\nabla \dot{\mathbf{u}} + \nabla \dot{\mathbf{u}}^T)$$

where σ_y is the yield stress and the equivalent strain rate $\dot{\bar{\boldsymbol{\epsilon}}}$ is

$$\dot{\bar{\boldsymbol{\epsilon}}} = \sqrt{\frac{2}{3}(\mathbf{d} : \mathbf{d} + I_d^2)}$$

where $I_d = \text{tr}(\mathbf{d})$, considering the incompressibility of the material in plane stress. From these relations, the yield criterion and the postulate of maximum dissipation we can write the relation:

$$\boldsymbol{\sigma} = 2\mu(\mathbf{d} + I_d \mathbf{I})$$

with $\mu = \sigma_y / 3\dot{\epsilon}$ and \mathbf{I} being the second order unity tensor, so the tangent constitutive tensor can be written as

$$\mathbb{C} = \frac{\partial \boldsymbol{\sigma}}{\partial d} = \frac{\partial^2 D_p}{\partial d \partial d} = 2\mu(\mathbf{I} \otimes \mathbf{I} + \mathbb{I}) - \frac{1}{3\mu\dot{\epsilon}^2} \boldsymbol{\sigma} \otimes \boldsymbol{\sigma}$$

where $\mathbb{I}_{ijkl} = \frac{1}{2}(\delta_{ik}\delta_{jl} + \delta_{il}\delta_{jk})$.

With these at hand, now we state the upper bound problem as a minimisation scheme as

$$\gamma^c = \Pi_p(\mathbf{v}) / \Pi_t(\mathbf{v}) = \min_{\dot{\mathbf{u}} \in Y} [\Pi_p(\dot{\mathbf{u}}) / \Pi_t(\dot{\mathbf{u}})]$$

where γ^c is the true collapse multiplier, \mathbf{v} and $\dot{\mathbf{u}}$ are the collapse and arbitrary velocity fields, respectively; as well as $\Pi_p(\dot{\mathbf{u}})$ and $\Pi_t(\dot{\mathbf{u}})$ denoting the total plastic (internal) work and the external work. We now normalize the solution to obtain a load vector which produces a unit external work, so we define the *reduced* space \bar{Y} as:

$$\bar{Y} = \{\dot{\mathbf{u}} \in Y \mid \Pi_t(\dot{\mathbf{u}}) = 1\}$$

and therefore the problem reduces to

$$\gamma^c = \min_{\dot{\mathbf{u}} \in \bar{Y}} \Pi_p(\dot{\mathbf{u}})$$

3. THE UPPER BOUND SOLUTION

We consider a finite element discretization of the body over a reduced space \bar{Y}_H so that the multiplier can be rewritten as

$$\gamma^c = \Pi_p(\mathbf{v}_H) = \min_{\dot{\mathbf{u}} \in \bar{Y}_H} \Pi_p(\dot{\mathbf{u}}) \quad \text{so that} \quad \gamma^c \leq \gamma_H$$

The constrained minimisation produces a set of equations that lead to a Newton-Raphson solution technique, provided the singularity of the stiffness is taken care of, and an initial velocity vector can be computed, in this case, as the normalized elastic finite element solution. Y_H denotes the corresponding solution space:

$$Y_H = \{\dot{\mathbf{u}} \in Y \mid \dot{\mathbf{u}} = \sum \dot{\mathbf{u}}_a N_a\}$$

for a given set of finite element shape functions N_a over a mesh with $a = 1, \dots, n$ nodes. Consider also the *reduced* space \bar{Y}_H :

$$\bar{Y}_H = \{\dot{\mathbf{u}} \in Y_H \mid \Pi_t(\dot{\mathbf{u}}) = 1\}$$

A Lagrange minimization technique is used to compute a velocity field \mathbf{v}_H that produces the least internal plastic work at imminent collapse. The Lagrange solution takes the form

$$\mathbf{T}(\dot{\mathbf{u}}) - \lambda \mathbf{H}(\dot{\mathbf{u}}) = 0$$

where $\mathbf{T}(\dot{\mathbf{u}}) = \int_{\Omega} \mathbf{B}^T \boldsymbol{\sigma} d\Omega$ and $\mathbf{H}(\dot{\mathbf{u}}) = \partial \Pi_t / \partial \dot{\mathbf{u}}$. The Newton-Raphson procedure yields an iterative process based on the step expression

$$\mathbf{K}_k \Delta \dot{\mathbf{u}} = \lambda_{k+1} \mathbf{F} - \mathbf{T}(\dot{\mathbf{u}}_k)$$

where $\lambda_{k+1} = \Pi_p(\dot{\mathbf{u}}_k)$, \mathbf{F} is the external force vector and \mathbf{K}_k is the tangent matrix. Because of the singularity of the tangent matrix, a special treatment is given to the solution construct which produces a reduced number of degrees of freedom when solving the equilibrium equation.

4. THE LOWER BOUND EVALUATION

Consider a very fine mesh Y_h in figure 1.b, obtained by enriching Y_H shown in figure 1.a, by higher order polynomials or element subdivision. By construction $Y_H \subset Y_h$ and we will assume that the solution in Y_h is sufficiently accurate, that is

$$\gamma^c \simeq \gamma_h \equiv \Pi_p(\mathbf{v}_h) = \min_{\dot{\mathbf{u}} \in \bar{Y}_h} \Pi_p(\dot{\mathbf{u}}) \quad (1)$$

where the reduced space \bar{Y}_h is as before $\bar{Y}_h = \{\dot{\mathbf{u}} \in Y_h \mid \Pi_t(\dot{\mathbf{u}}) = 1\}$.

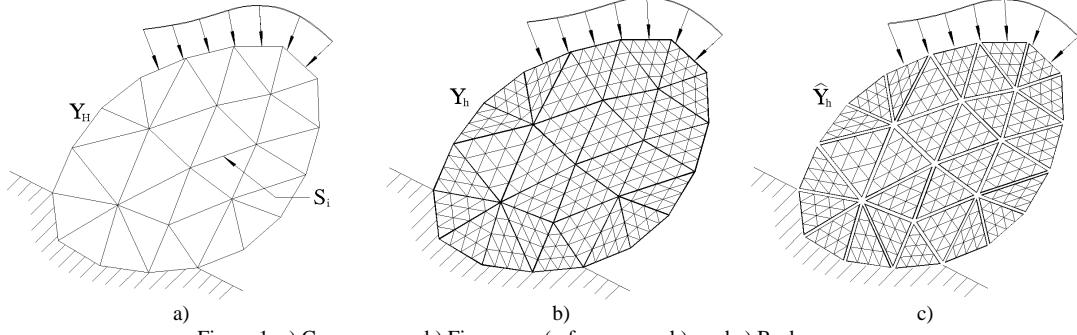


Figure 1. a) Coarse space; b) Fine space (reference mesh); and c) Broken space.

Consider that the fine space Y_h of figure 1.b) has the *broken* space \hat{Y}_h in figure 1.c) where continuity across the edges of Y_H macroelements is not enforced. Note that $Y_h \subset \hat{Y}_h$. To restore continuity we introduce the edge forces \mathbf{q}

$$b(\mathbf{q}, \dot{\mathbf{u}}) = \int_{S_i} \mathbf{q} \cdot \llbracket \dot{\mathbf{u}} \rrbracket dl$$

where $\llbracket \dot{\mathbf{u}} \rrbracket$ denotes the jump of $\dot{\mathbf{u}}$ across the interval edges S_i . Then

$$Y_h = \{\dot{\mathbf{u}} \in \hat{Y}_h \mid b(\mathbf{q}, \dot{\mathbf{u}}) = 0, \forall \mathbf{q}\}$$

The reduced space \bar{Y}_h is now

$$\bar{Y}_h = \{\dot{\mathbf{u}} \in \hat{Y}_h \mid \Pi_t(\dot{\mathbf{u}}) + b(\mathbf{q}, \dot{\mathbf{u}}) = 1, \forall \mathbf{q}\}$$

Note that the condition $\Pi_t(\dot{\mathbf{u}}) = 1$ is obtained by taking $\mathbf{q} = 0$. The minimization (1) is now rewritten with the help of the Lagrangian

$$\alpha_h(\dot{\mathbf{u}}, \mathbf{q}, \gamma) = \Pi_p(\dot{\mathbf{u}}) + \lambda_h [1 - \Pi_t(\dot{\mathbf{u}}) - b(\mathbf{q}, \dot{\mathbf{u}})]$$

and based on duality theory as in [3] we have:

$$\gamma_h = \min_{\dot{\mathbf{u}} \in \bar{Y}_h} \max_{\lambda_h, \mathbf{q}} \alpha_h(\dot{\mathbf{u}}, \mathbf{q}, \lambda_h)$$

leading to

$$\gamma_h \geq \max_{\mathbf{q}} \min_{\dot{\mathbf{u}} \in \bar{Y}_h} \max_{\lambda_h} \alpha(\dot{\mathbf{u}}, \mathbf{q}, \lambda_h) \geq \min_{\dot{\mathbf{u}} \in \bar{Y}_h} \max_{\lambda_h} \alpha(\dot{\mathbf{u}}, \mathbf{P}_H, \lambda_h) \equiv \hat{\gamma}_h \quad (2)$$

This represents a lower bound to the collapse multiplier γ^c . The term \mathbf{P}_H in (2) represents a particular choice of \mathbf{q} to be evaluated in the coarse mesh. The determination of the edge forces \mathbf{q} in this implementation is accomplished by the *flux equilibration method* initially proposed in [4]. A simpler expression for $\hat{\gamma}_h$ is obtained by first defining the *augmented* external force term

$$\hat{\Pi}_t(\dot{\mathbf{u}}) = \Pi_t(\dot{\mathbf{u}}) + b(\mathbf{P}_H, \dot{\mathbf{u}})$$

and the reduced broken space as

$$\hat{\hat{Y}}_h = \{\dot{\mathbf{u}} \in \hat{Y}_h \mid \hat{\Pi}_t(\dot{\mathbf{u}}) = 1\} \quad (3)$$

Hence $\hat{\gamma}_h$ is now

$$\hat{\gamma}_h \equiv \Pi_p(\hat{\mathbf{v}}_h) = \min_{\dot{\mathbf{u}} \in \hat{\hat{Y}}_h} \Pi_p(\dot{\mathbf{u}})$$

Despite the fact that condition (3) seems to tie up the solution of the local problems, they can in fact be solved individually. To show this consider each macroelement $e = 1, \dots, m_H$ in turn, where m_H is the number of elements in the coarse mesh. Consider the corresponding *reduced* space $\bar{Z}_h^e = \{\dot{\mathbf{u}}^e \in Z_h^e \mid \hat{\Pi}_t^e(\dot{\mathbf{u}}^e) = 1\}$.

Here, $\dot{\mathbf{u}}^e$ is the velocity field within the local domain, and $\hat{\Pi}_t^e(\dot{\mathbf{u}}^e)$ denotes the work done by the forces acting on the edges of element e . We now define the local (elemental) minimizers $\hat{\gamma}_h^e$ as

$$\hat{\gamma}_h^e \equiv \min_{\dot{\mathbf{u}}^e \in Z_h^e} \Pi_p^e(\dot{\mathbf{u}}^e) = \Pi_p^e(\hat{\mathbf{v}}_h^e)$$

Proposition: the minimizer $\hat{\gamma}_h$ is

$$\hat{\gamma}_h = \min_{e=1, \dots, m_h} \hat{\gamma}_h^e \equiv \hat{\gamma}_h^E$$

Proof: Consider any $\dot{\mathbf{u}}_h \in \hat{Y}_h$ and let $\dot{\mathbf{u}}_h^e$ denote its restriction to macro-element e . With this notation

$$\Pi_p(\dot{\mathbf{u}}_h) = \sum_e \Pi_p^e(\dot{\mathbf{u}}_h^e) \quad \text{with condition} \quad \hat{\Pi}_t(\dot{\mathbf{u}}_h) = \sum_e \hat{\Pi}_t^e(\dot{\mathbf{u}}_h^e) = 1$$

Then

$$\begin{aligned} \Pi_p(\dot{\mathbf{u}}_h) &= \sum_e \Pi_p^e(\dot{\mathbf{u}}_h^e) = \sum_e \hat{\Pi}_t^e(\dot{\mathbf{u}}_h^e) \Pi_p^e\left[\frac{\dot{\mathbf{u}}_h^e}{\hat{\Pi}_t^e(\dot{\mathbf{u}}_h^e)}\right] \\ &\geq \sum_e \hat{\Pi}_t^e(\dot{\mathbf{u}}_h^e) \Pi_p^e(\hat{\mathbf{v}}_h^e) \end{aligned} \quad (4)$$

$$\geq \hat{\gamma}_h^E \sum_e \hat{\Pi}_t^e(\dot{\mathbf{u}}_h^e) \geq \hat{\gamma}_h^E \quad (5)$$

This last inequality implies that in the broken problem the deformation localises in the weakest element. A lower bound, from the proof above, can be better computed from expression (4), that is

$$\hat{\gamma}_h = \sum_e \hat{\Pi}_t^e(\dot{\mathbf{u}}_h^e) \Pi_p^e(\hat{\mathbf{v}}_h^e)$$

This last expression corresponds to an integral approach, incorporating each elemental contribution to the lower bound, as opposed to the local approach which is based on a single element contribution, described by expression (5). The integral approach gives the best results, which are described thereafter in the present paper.

5. ADAPTIVITY ISSUES

The implementation of the adaptive procedure used in this work is based on a h -refinement method by element subdivision, as summarized in [5]. The upper and lower bounds produce what is known as the *bound gap* which can be determined as the sum of the differences between the contributions of the upper and the lower bound on a local, element-by-element basis. This can be summarized as

$$g = \sum_e g_e \quad \text{with} \quad g_e = \Pi_p^e(\dot{\mathbf{u}}_H^e) - \hat{\Pi}_t^e(\dot{\mathbf{u}}_h^e) \Pi_p^e(\hat{\mathbf{v}}_h^e)$$

so that the elemental contribution to the total gap is used as the *adaptivity indicator*, using the *maximum contribution* criteria, that is: refine those elements where $g_e \geq \gamma \cdot \eta$ for some $0 < \gamma < 1$ chosen by the user, with $\eta = \max_e g_e$. The refinement process uses a set of rules to deal with hanging nodes on non-conforming elements, which constitutes a convenient, simple re-meshing strategy.

6. NUMERICAL RESULTS

An end-loaded wide tapered cantilever beam in plane stress as that presented in [6] is used for a brief discussion of the results. The figure 2.a) shows the case problem with the coarse initial mesh. An intermediate step in the adaptive process is depicted in figure 2.b). The final adaptively refined mesh of the solution is shown in figure 2.c) clearly describing the plastic regions where slip-lines are expected to occur.

In figure 3.a) a plot of the upper and lower bounds progression for adaptive refinement is presented, indicating the average predictor progression. Meanwhile, in figure 3.b) the rate of convergence of the bound gap and the bounds errors are depicted. Similar results to those of figure 3.a) were observed for the case of uniform refinement, with the evident higher processing drag of the latter.

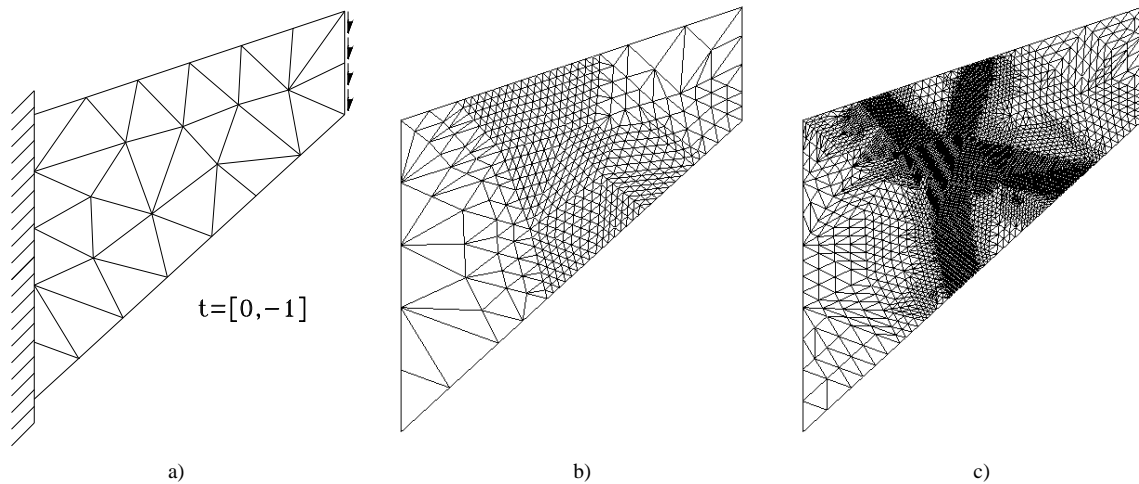


Figure 2. An adaptive refinement sequence

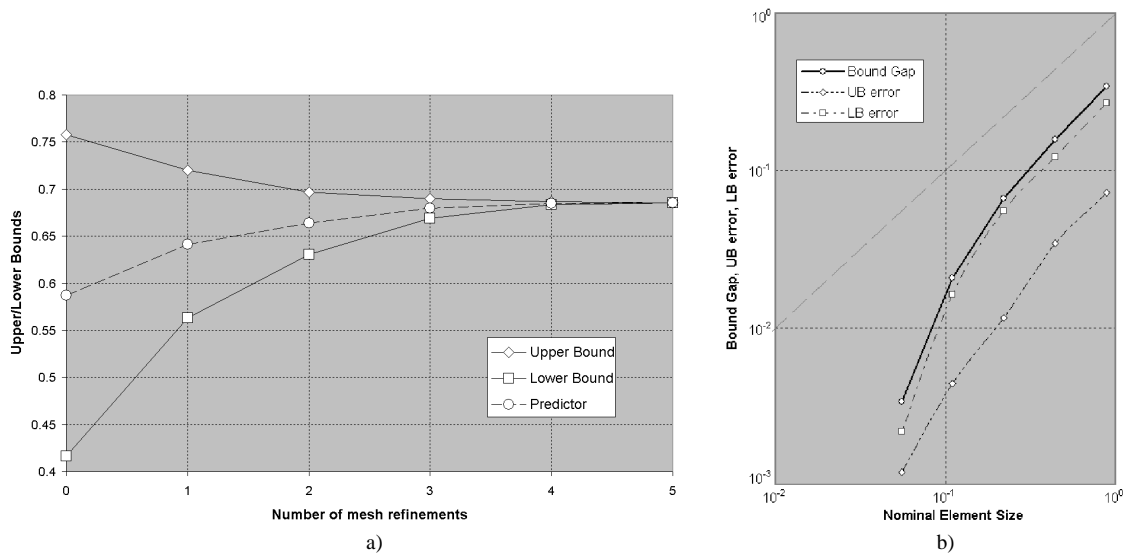


Figure 3. Upper and lower bounds and rate of convergence plots

7. CONCLUSION

An innovative solution procedure to the limit state analysis problem in plane stress for rigid-plastic Von Mises materials is presented. The numerical results show a good performance in terms of the quality of the output and processing time. Extensions to new modelling conditions are being considered for future research.

ACKNOWLEDGEMENT

This research work is sponsored by CONACYT Mexico, under scholarship reference number: 161990/170856.

REFERENCES

- [1] Jirazek M., Bazant Z. Inelastic Analysis of Structures. John Wiley & Sons, Ltd., Chichester, 2001.
- [2] Lubliner J. Plasticity Theory. Macmillan Publishing Company, New York, 1990.
- [3] Christiansen, E. Computation of Limit Loads. Intl. J. Numerical Methods in Eng., Vol.17, 1981, 1547-1570.
- [4] Ladeveze P., Leguillon D. Error Estimate Procedure in the Finite Element Method and Applications. SIAM Journal on Numerical Analysis, Vol. 20, Issue 3, 1983, 485-509.
- [5] Haegland B., Skaflestad B. A Survey of Some Methods for Moving Grid and Grid Adaptation. Numerics No. 2, Norwegian University of Science and Technology, 2002.
- [6] Peraire J., Ciria H. Computation of Upper and Lower Bounds in Limit Analysis using Second-order Cone Programming and Mesh Adaptivity. MSc Thesis, Massachusetts Institute of Technology, 2004.